LIMNOLOGY
and
OCEANOGRAPHY: METHODS

Limnol. Oceanogr.: Methods 9, 2011, 340–347

Simple, robust eddy correlation amplifier for aquatic dissolved oxygen and hydrogen sulfide flux measurements

Daniel F. McGinnis[1,2], Sergiy Cherednichenko[1], Stefan Sommer[1], Peter Berg[3], Lorenzo Rovelli[1], Ralf Schwarz[1], Ronnie N. Glud[2,4,5], and Peter Linke[1]*

[1]IFM-GEOMAR, Leibniz Institute of Marine Sciences, RD2 Marine Biogeochemistry, Kiel, Germany D-24148
[2]Southern Danish University, Institute of Biology and Nordic Center for Earth Evolution (NordCee), 5230 Odense M, Denmark
[3]Department of Environmental Sciences, University of Virginia, Charlottesville, VA 22904-4123
[4]Greenland Climate Research Centre (Co. Greenland Institute of Natural Resources), Kivioq 2, Box 570, 3900 Nuuk, Greenland
[5]Scottish Association for Marine Science, Dunstaffnage Marine Laboratory, PA37 1QA, Dunbeg, Scotland

Abstract

The aquatic application of the eddy correlation (EC) technique is growing more popular and is gradually becoming a standard method for resolving benthic O_2 fluxes. By including the effects of the local hydrodynamics, the EC technique provides greater insight into the nature of benthic O_2 exchange than traditional methods (i.e., benthic chambers and lander microprofilers). The growing popularity of the EC technique has led to a greater demand for easily accessible and robust EC instrumentation. Currently, the EC instrumentation is limited to two commercially available systems that are still in the development stage. Here, we present a robust, open source EC picoamplifier that is simple in design and can be easily adapted to both new and existing acoustic Doppler velocimeters (ADV). The picoamplifier has a response time of < 0.1 ms and features galvanic isolation that ensures very low noise contamination of the signal. It can be adjusted to accommodate varying ranges of microelectrode sensitivity as well as other types of amperometric microelectrodes. We show that the extracted flux values are not sensitive to reduced microelectrode operational ranges (i.e., lower resolution) and that no signal loss results from using either a 16- or 14-bit analog-to-digital converter. Finally, we demonstrate the capabilities of the picoamplifier with field studies measuring both dissolved O_2 and H_2S EC fluxes. The picoamplifier presented here consistently acquires high-quality EC data and provides a simple solution for those who wish to obtain EC instrumentation. The schematic of the amplifier's circuitry is given in the Web Appendix.

The eddy correlation (EC) technique in aquatic systems is becoming a more commonly applied method for determining O_2 fluxes at boundary-layer interfaces. The advantage of the EC technique is that it noninvasively resolves constituent fluxes in high-temporal resolution and can do so at study sites where it is not feasible to deploy benthic chambers or microprofilers (e.g., coral reefs or rocky bottoms). Furthermore, the EC measurements document the natural hydrodynamics, and thus shed new light on the highly intermittent nature of benthic fluxes. The technique has since been applied by various researchers in lakes (Brand et al. 2008), rivers (McGinnis et al. 2008; Lorrai et al. 2010), shallow coastal regions (Berg et al. 2003; Kuwae et al. 2006; Berg and Huettel 2008), deep-ocean sediments (Berg et al. 2009), hard-bottom substrates (Glud et al. 2010), sea grass beds (Hume et al. 2011), and has now been extended to measure H_2S fluxes in the Baltic Sea (this work). Whereas the EC technique has a great potential for a wide range of applications, the number of users is still relatively limited. One of the largest challenges is acquiring reliable EC equipment.

The concept of the EC measurement is simple—simultaneously obtaining temporally high-resolution measurements of

*Corresponding author: E-mail: danielm@biology.sdu.dk

Acknowledgments

The authors would like to express their gratitude to the members of the mechanical workshop at the Technik- und Logistikzentrum at IFM-GEOMAR, and for the technical support provided by Bernhard Bannert, Asmus Petersen, Wolfgang Queisser, and Matthias Türk. We would also like to thank the captain and crew of RV *Alkor* (AL352). Furthermore, we are grateful to Anni Glud for providing the microelectrodes used in this study, and the two anonymous reviewers for providing improvements to the manuscript. The project (DFM, RG) was financially supported by the National Environmental Research Council (NERC; NE/F012691/1), the Commission for Scientific Research in Greenland (KVUG; GCRC6507), the European Union's Seventh Framework Programme HYPOX (grant agreement n° 226213), and the cluster of excellence 80/1 "The Future Ocean" funded by the German Science Foundation. PB was financially supported by the US National Science Foundation (Chemical Oceanography Program OCE 0536431).

DOI 10:4319/lom.2011.9.340

two parameters—the vertical velocity and the dissolved constituent (from here on referred to as O_2 unless otherwise specified) in the same measurement location (measurement volume; Fig. 1A). The determined fluxes are derived from the signals arising from seafloor exchange in an upstream area of ~10-100 m^2 (Berg et al. 2007). The O_2 concentration must be measured with fast responding microelectrodes (<0.2 to 0.3 s) and a fast, robust picoamplifier (Berg et al. 2003; McGinnis et al. 2008; Lorrai et al. 2010).

Whereas the O_2 EC technique is gradually becoming a standard flux measurement approach, there still exists a deficit of reliable, affordable 'off-the-shelf' EC equipment. At the time of this publication only two commercial manufacturers provide complete O_2 EC systems, however, neither of these systems have a proven track record. Therefore, we developed a simple, robust amplifier in an open-source effort between various researchers with the goal that the amplifier design is available for free to interested users. Our amplifier is highly customizable for both varying microelectrode ranges and can be used with different amperometric electrodes. The amplifier itself is a single component and can be easily adapted to existing ADVs with an analog input. The functional circuitry is galvanically isolated and features very low noise which is necessary for indoor flumes subject to 50/60Hz electrical noise contamination. The amplifier can be easily built in-house by personnel with qualified electronics training or by outside manufacturers and will increase the availability of EC systems for the scientific community.

The main technical features of the amplifier include the following: Adjustable sensor polarization, gain, and voltage-offsets—can use any type of amperometric microelectrode with polarization potentials within ±1.2 V; ability to measure in burst or continuous mode; clean, unfiltered acquisition of sensor data; cutoff filtering and response time of signal well above the frequency range of contributing eddies; galvanic isolation; self-contained, plug-and-play design adaptable to existing ADVs with analog inputs.

In this article, we describe the amplifier concept and design, test the response time, present (briefly) the sensor mounting and housing, and perform a sensitivity analysis evaluating potential loss of flux due to limitations in sensor ranges and analog-to-digital conversion. Finally, results are shown from field tests in a local river (O_2) and the Baltic Sea (H_2S).

Materials and procedures

The complete EC system consists of an ADV (Fig. 1A), amplifier and housing, sensors and mount, a deployment frame, and associated battery housings, cables, etc. Several configurations exist and most of these details are published (see references above). We focus here on the picoamplifier.

Electronics

Fig. 2A shows the top and bottom photo of the amplifier and the schematic overview (Fig. 2B – See Web Appendix for complete schematics). The components are mounted on a 3 × 7 cm board using high-quality components. The amplifier can operate between 9 to 18 V input power, but other voltages can be adapted. The average power consumption is 50 mA at 12 V. The output voltage is ± 14 V, which offers a wide range of applications. The galvanic isolation separates the measurement current from the output current and therefore avoids feedback and reduces noise contamination of the signal.

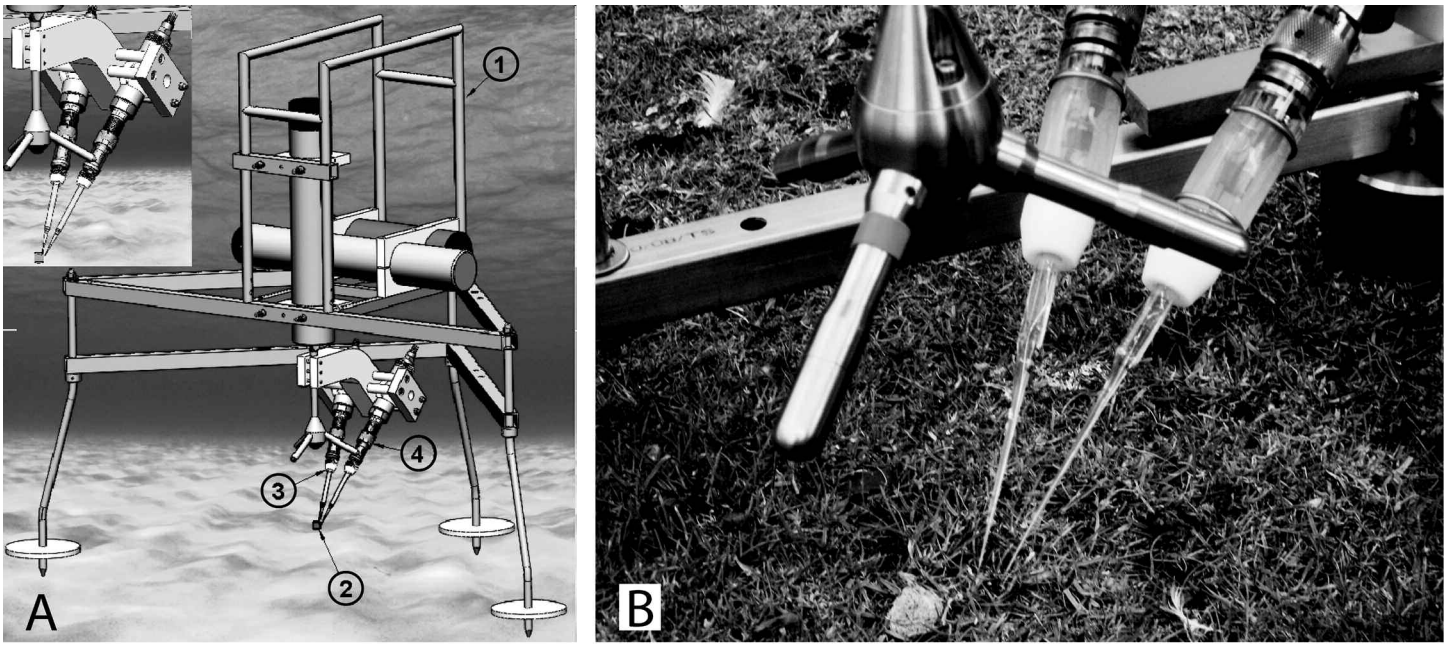

Fig. 1. A) Eddy correlation system shown on an ROV-deployable frame. 1) frame, 2) measurement volume, 3) sensor and sensor holder and 4) amplifier housing and connector. B) Dual O_2 sensor deployed on the same ADV.

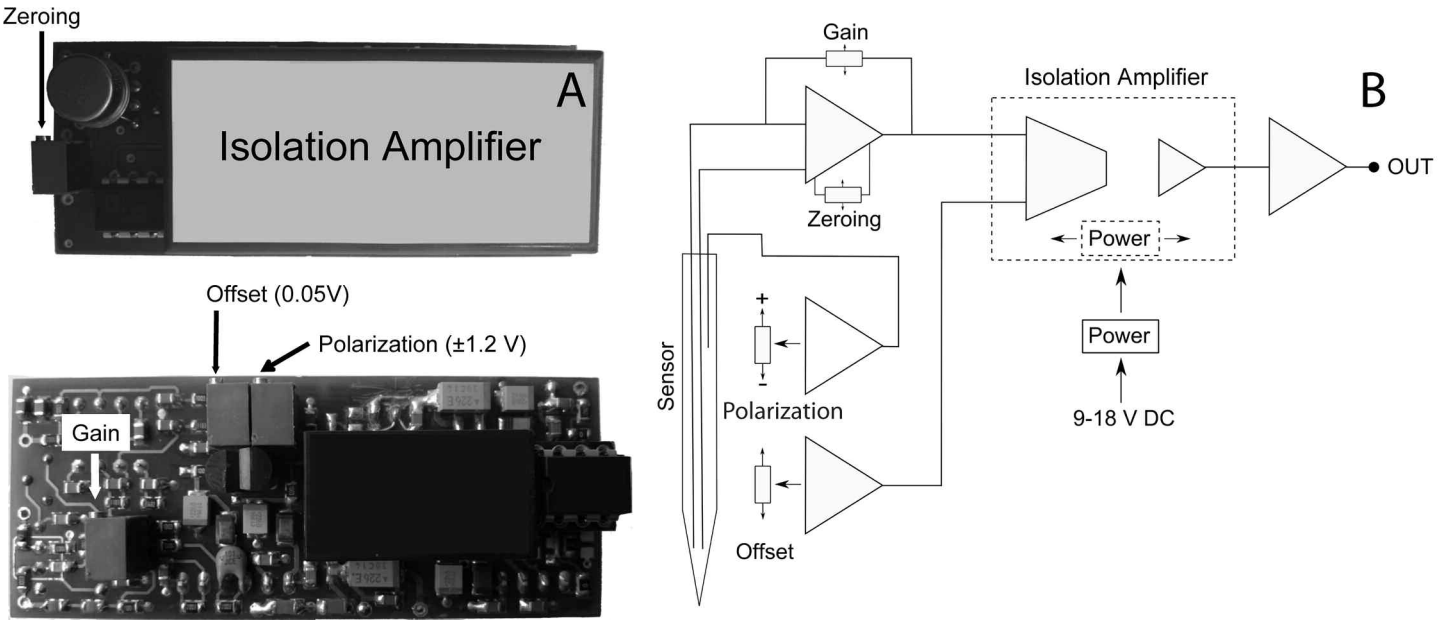

Fig. 2. A) Photograph of the galvanically isolated picoamplifier. Amplifier features zeroing control, adjustable gain for 'tuning' high sensor range for optimal output voltage, offset voltage adjustment (e.g., set zero signal to 0.05 V to prevent off scale readings), and finally adjustable polarization. B) Simple schematic drawing of the various units within the amplifier.

Adjustable gain

As the pA output of every microelectrode is different (e.g., in a test batch of 10 microelectrodes the output values for 0% O_2 saturation ranged from 3-20 pA while 100% ranged from 54-220 pA), the amplifier is equipped with an adjustable range (gain) setting. This allows the 'tuning' of the system to optimize the measurement voltage output. Furthermore, the voltage output can also be specially adjusted for the system in which measurements will take place, for example in a system with very low oxygen concentration the range can be enlarged to increase measurement resolution.

Adjustable polarization

The amplifier is designed to be used with any sensors with polarization potentials between ± 1.2 V, however currently only O_2 and H_2S sensors are fast enough for EC application. These sensors require different polarization voltages for O_2 (–0.78 V) and H_2S (+0.08 V) (Revsbech, 1989; Kuhl et al. 1998).

Offset

The offset setting allows the user to adjust the lower voltage output that corresponds to the 0 µmol L^{-1} input signal. This helps to prevent potential off-scale reading in the event of sensor drift.

Laboratory testing

The response of the amplifier to input signals ranging from 1 to 100 Hz was tested using a DC square wave generator. This essentially tests the amplifier's ability to resolve realistically sized fluctuations. The generated signal was recorded through two separate channels: one was connected directly to an oscilloscope (reference signal), whereas the other one was first sent through the amplifier. The amplifier signal was then compared with the reference signal to determine response time and signal loss/cutoff.

Amplifier housing

The amplifier is housed within a stainless steel casing (Fig. 3) with a pressure rating of 6000 m. The system described below utilizes impulse connectors between the sensor and the amplifier with a silicon oil-filled sensor holder for pressure compensation (plans available upon request). The impulse connector is pressure rated to 3500 m; however sensor holders using Kemlon connectors (rated for 6000 m) have been used and are available (plans available upon request).

EC system

The analog output from the amplifier is connected to the ADV analog input with a shielded cable and a 5-pin impulse connector. Different types and qualities of connectors and cables exist with a trade-off between availability, price, and signal quality that goes beyond this study. The Vector used in this study is equipped with a Nortek-supplied end-bell with two analog inputs (5-pin each) and an 8-pin external power/RS-422 connection. The system allows a maximum of two sensors to be simultaneously deployed (Fig. 1). Power for the ADV is supplied by batteries installed in the ADV housing or with an external battery canister, and power for the amplifiers is supplied by a separate, external battery source (Fig. 1A). With the 4GB memory available on the Nortek ADV, this configuration allows over 10 d of continuous data collection at 64 Hz (assuming six 13.5V 50 Wh batteries for the ADV). With 20 D cell batteries, a single amplifier can be

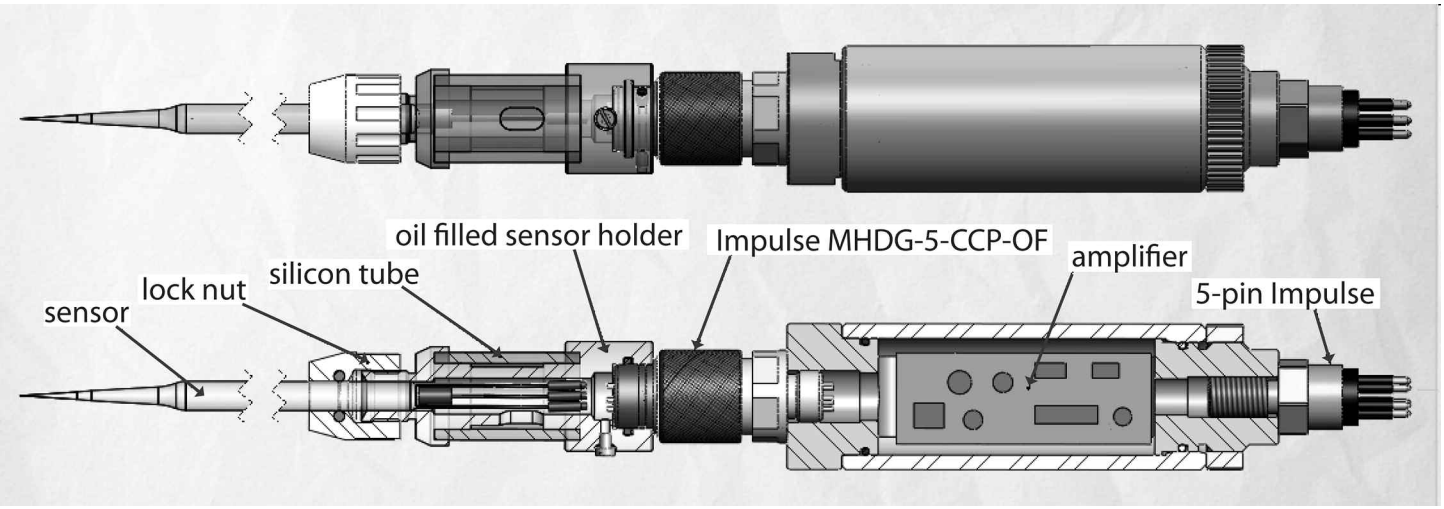

Fig. 3. Amplifier housing, sensor, and sensor holder with impulse connector. Systems using other deep-rated connectors have also been designed and applied.

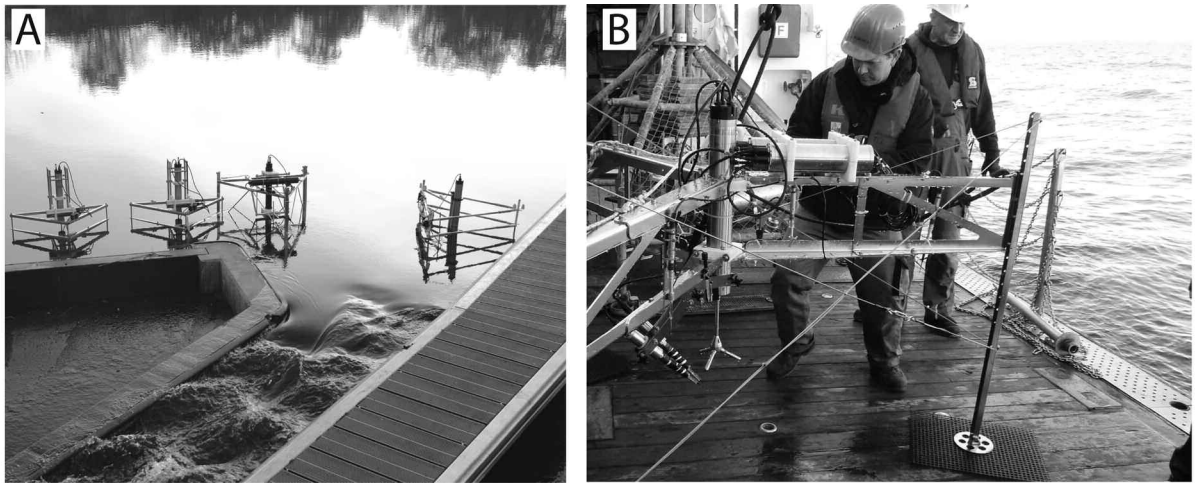

Fig. 4. Field test deployments. A) O_2 flux test in the Schwentine River. B) Deployment of H_2S sensors in the Baltic Sea mounted on a Unisense frame.

operated from 7 to 9 d. For further details on deployment, see Berg et al. (2003), Berg and Huettel (2008), and McGinnis et al. (2008). The EC equipment can be mounted on various frames optimized for different environmental conditions (Fig. 4) including the IFM-GEOMAR frame for ROV deployments (Fig. 1A).

Flux analysis

The constituent (C) fluxes (F) are expressed as $F = V_Z\ C$ (mass area^{-1} time^{-1}), where the vertical velocity V_Z and constituents can be broken up into their mean and turbulent fluctuation $V_Z = \overline{V}_Z + V_Z'$ and $C = \overline{C} + C'$ (Berg et al. 2003; Lee et al. 2004). The fluxes are calculated from raw velocity and dissolved constituent data using a self-developed software program (McGinnis unpubl. data). For simplicity, the mean and fluctuation are defined and extracted using linear detrending (see Lee et al. 2004) over generally 2 to 2.5 min windows. This time window is selected as it includes all contributing eddies (up to ~100 s) while excluding larger scale, non-turbulent contributions (McGinnis et al. 2008; Lorrai et al. 2010). Due to the turbulent nature of the fluxes (i.e., the large degree of flux variability), they are averaged into 15 min time windows (Berg et al. 2009).

Sensitivity to lower grade AD converter

The following procedure is used to investigate potential flux signal loss due to the 16-bit AD converter. We developed an EC simulation program that models the O_2 measurement from the tip of the electrode through the amplifier and finally the 16-bit converter in the Vector. The assumption is that the O_2 concentrations in the original data set are those that will be actually measured in the water column by the modeled EC. This analysis extends to the sensitivity of potentially limited ranges of microelectrodes.

Procedure:

1. O_2 measured is converted to pA (0–~300) with a linear relation.
2. pA range is converted to voltage (0–5) where 4 V is 100% O_2 saturation.
3. Volts are converted to bits (digitized).
4. Bits are converted to an integer, which is now a step function of voltage.
5. O_2 'processed' is calculated from bits (linear relation).
6. Fluxes are extracted from 'processed' O_2 data.

Freshwater O_2 tests

Two field tests were conducted in the Schwentine River in Kiel, Germany (Fig. 4A). This is a shallow (~70 cm) dammed river. The EC devices were positioned near the spillway where the water velocity was relatively constant. The first test was in 19 June 2009 in which two sensors were deployed simultaneously with a single ADV. The second test was conducted in November 2009, however one of the sensors failed.

Baltic Sea H_2S test

The H_2S field test was conducted in the anoxic deepwater of the Baltic Sea in June 2010 aboard RV *Alkor* during cruise AL355 (Fig. 4B). The system was deployed in the Eastern Gotland Basin at 192 m depth and collected data for nearly 24 h (15 Jun 16:48 – 16 Jun 16:28). The deployment was approximately 50 km west of Ventspils, Latvia (57°18.71′ 20°32.95′). Two H_2S microelectrodes were attached on the EC equipment; however one of them malfunctioned as the system was deployed.

Assessment

Amplifier frequency range

While the size distribution and time scales of the vertical eddies depend on local hydrodynamics (see Lorrai et al. 2010), for field applications the frequency of the flux contributing eddies are generally in the range of 0.01 – 1 Hz (1 – 100 s) (Berg et al. 2003; McGinnis et al. 2008). The fastest eddies we should ever have to resolve are slower than about 3-5 Hz (Kuwae et al. 2006; Lorrai et al. 2010). Therefore, it is crucial that the amplifier can resolve the smallest eddy with no signal loss due to cutoff or response time. It was found that nearly independent of input frequency, the amplifier generally had a response time of < 0.1 ms. There is no signal loss due to the cutoff frequency (50 Hz) from low frequencies up to 20 Hz. Therefore, the amplifier is fully capable of resolving the complete spectrum of flux contributing eddies.

Noise analyses

Noise in the amplifier is due to external/internal electrical issues, sensor imperfections, and perhaps loose or moist connections. This noise is random (white) and cancels out in the flux calculations. However, it is obviously desirable to minimize the noise in the measurement system, especially in oligotrophic systems where fluxes can be below 1 mmol m^{-2} d^{-1}.

The noise analysis is simply defined as the difference of neighboring data points $C_{i+1} - C_i$, and is performed on the unfiltered, raw 64 Hz data— much faster than the fastest eddies. The data are plotted in a normalized histogram (Fig. 5). The left 3 panels (Fig. 5A-C) are from the EC systems shown in Fig. 4A in the Schwentine River. These have surprising low noise considering the environment where they are deployed (near electrical cables and not completely submersed). The H_2S EC deployed in the Baltic Sea also shows very low noise in the data. Furthermore, the noise is approximately evenly distributed (Gaussian) reflecting "white noise," which does not interfere with the flux values.

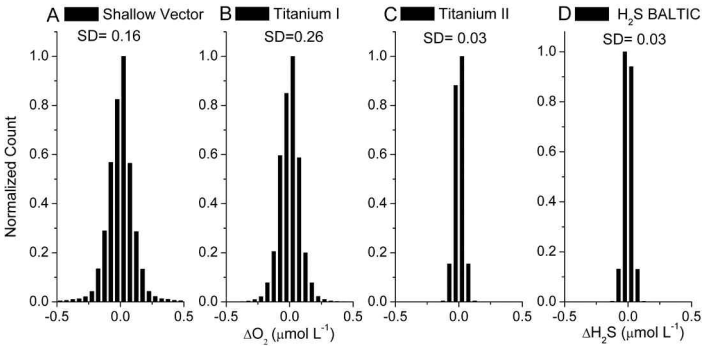

Fig. 5. A, B, C) Noise from three simultaneously shallow-deployed EC systems over the entire deployments (<1 m Schwentine River; Fig. 4A). D) H_2S noise over the ~16 h deployment in the Baltic Sea (192 m; Fig. 4B).

n-bit analog to digital conversion and sensor range

The Nortek Vector utilizes a 16-bit AD converter. Obviously, there is a risk that loss of the constituent fluctuations in the analog-to-digital conversion will affect the flux calculations. Therefore, we evaluate this process by using a computer simulation to step down the bits and recalculate the fluxes to determine when and how much of the flux signal may be lost (Table 1, Fig. 6).

Two data sets were used in the analyses covering the broad range of fluxes and conditions that can be encountered: the Schwentine River data (O_{2avg} = 212 µmol L^{-1}, V_{avg} = 5.4 cm s^{-1}, $Flux_{avg}$ = 30.4 mmol m^{-2} d^{-1}) and the deep-sea data from Berg et al. (2009) (O_{2avg} = 59 µmol L^{-1}, V_{avg} = 1.7 cm s^{-1}, $Flux_{avg}$ = –2.05 mmol m^{-2} d^{-1}). Table 1 lists the results of this analysis, as well as the corresponding converter and O_2 resolution assuming 0–250 µmol L^{-1} over the full scale (all available stored integers). Fig. 6A shows the dramatic reduction in resolution of measured O_2 as a function of AD converter bits; however, for both data sets no significant change was detectable in the fluxes down to 14 bits (Table 1; Fig. 6C). Surprisingly, for the Schwentine River data, only very small (<1%) errors were observed for bit conversions from 13 to 9. However, as expected for environments with low absolute O_2 exchange rates, the higher bit AD conversion is more critical. The EC data from a deep-sea site with low fluxes of 2.05 mmol m^{-2} d^{-1} (Berg et al. 2009) reveals a 2% error with the 13-bit converter, whereas the 10-bit proved to be too crude and led to a 64% error.

Similar to the AD converter grade analysis, the above results can also be directly related to the resolved microelec-

Table 1. Results of flux sensitivity to AD converter type and % of 16-bit full scale resolution for a high production flux (Schwentine River; 30.44 mmol m^{-2} d^{-1}) and low consumption flux (Berg et al. 2009; –2.05 mmol m^{-2} d^{-1}) system.

AD converter bits (2^n)	Steps in resolution	% of 16-bit range	O_2 resolution* µmol L^{-1}	Flux error† Schwentine %	Flux error† Berg et al. (2009) %
16	65536	100	0.0038	-	-
15	32768	50	0.0076	0.02	–0.32
14	16384	25	0.015	0.00	–0.81
13	8192	13	0.031	–0.18	–1.80
12	4096	6	0.061	0.34	4.22
11	2048	3	0.12	–0.49	–3.73
10	1024	2	0.24	–0.84	–63.8
9	512	0.8	0.49	0.61	89.4
8	256	0.4	0.98	12.0	–350

*Assumes O_2 range of 0 – 250 µmol L^{-1} over the entire converter resolution.
†Relative to the 16-bit AD converter fluxes

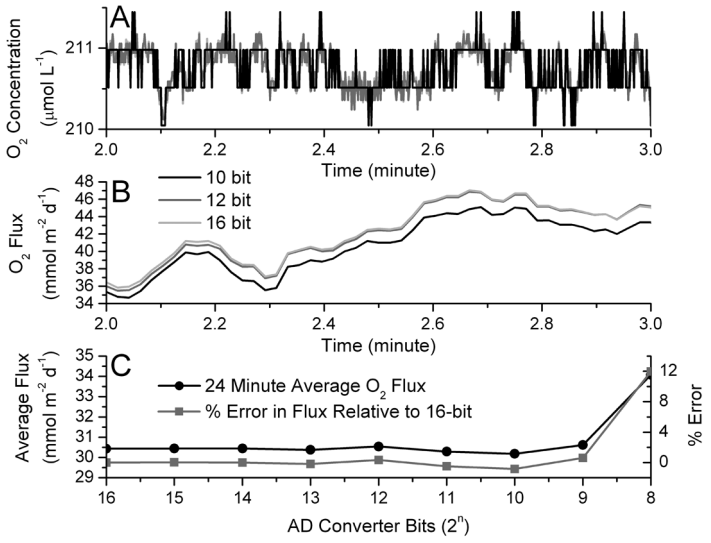

Fig. 6. Sensitivity to AD converter bits. The shown analysis was performed on 24 min of Schwentine River data, but for clarity only 1 min is shown. A) Resulting O_2 signal as a function of decreasing AD converter bits. B) O_2 fluxes calculated using the 16-, 12-. and 10-bit converters. C) Average flux results over 24 min and % error as a function of stepping down the AD converter bits from 16- to 8-bits in 1-bit decrements.

trode range, i.e., the effect of a decreased measurement range. For example, if the amplifier is set up for an O_2 microelectrode with a range of 0–300 pA (for 0–100% O_2 saturation corresponding to 0–65536 integers), then a sensor with a range from 0–40 pA would only be stored at a resolution equal to ~13% of the full scale or about 8200 integers (Table 1). This would be the same as a 13-bit AD converter over the full range (assuming no adjustable gain). As for the AD conversion, measurements resolving low fluxes (e.g., the data from Berg et al., 2009) are, as expected, more sensitive to the number of integers used to store the sensor readings.

While these two data sets appear to be relatively insensitive to sensor range and AD converter bits, they also demonstrate the added value of the adjustable gain feature of this amplifier. Furthermore, they also illustrate that auto-zeroing of the sensor signal is not essential for good performance.

Field testing: O_2

A field test was conducted in the Schwentine River during June 09 with two sensors connected to a single Vector (Fig. 1B). Results are shown in Fig. 7A. Generally, the two sensor fluxes compare well and reflect the same overall trend. Differences could be attributed to particles contacting the sensor tip. Both sensors verify the highly intermittent and variable nature of the fluxes in this eutrophic, shallow system, particularly the dramatic increase from consumption of –20 mmol m^{-2} d^{-1} at 10 min up to 120 mmol m^{-2} d^{-1} O_2 production at 22 min (Fig. 7A). However, the cumulative average of the fluxes quickly converge to a very close agreement and level off to about 30 mmol m^{-2} d^{-1}. These fluctuations are likely due to wind gusts driving turbulence and variable cloudiness (changing light for photosynthesis) during the testing in this shallow system. The effect of light is apparent in Fig. 7B during the Nov 2009 test at the same location.

In general, the O_2 flux follows the PAR signal. The deployment began at 13:30 and ran until 18:17. The day was overcast and sunset was about 3.5 h after the testing began. Fluxes remain fairly constant for the first hour at –40 mmol m^{-2} d^{-1} and then begin to decrease just around sunset. Fluxes leveled off at around –90 mmol m^{-2} d^{-1} in the final hour.

H_2S testing

H_2S EC measurements were performed in the anoxic waters of the Gotland Basin in the Baltic Sea. The fluxes were resolved with 2.5 min windows and averaged over 15 min (Fig. 8). The data show a continually decreasing H_2S_{aq} concentration ranging from about 47–39 µmol L^{-1} (Fig. 8A), however sensor drift cannot be excluded as no water samples were obtained for calibration. Current direction stayed nearly constant and velocity magnitude varied from ~3–8 cm s^{-1} (Fig. 8B).

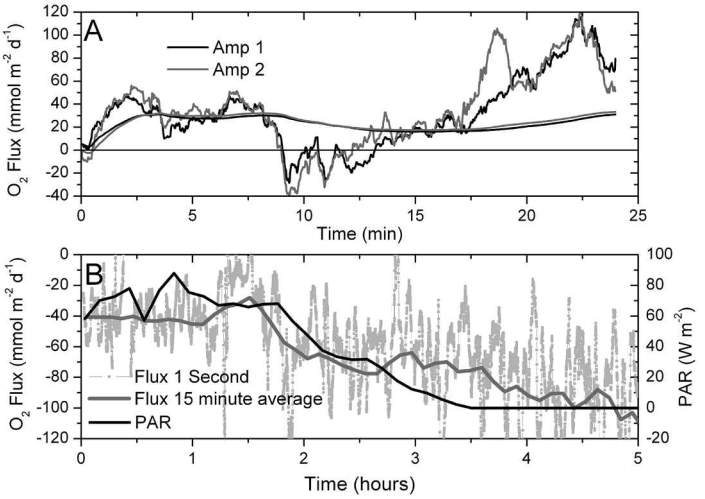

Fig. 7. A) Results of the Schwentine River test (June 2009) comparing two simultaneously deployed O_2 microsensors. The data are reported as fluxes every 1 s. O_2 fluxes were extracted with a 2-min window; the window was shifted 1 s and then resolved again. The instantaneous O_2 fluxes and cumulative averages (smoothed lines) are shown. B) Data from Nov 2009 Schwentine River test comparing oxygen flux and solar radiation (PAR). Light gray shows the fluxes every 1 s while solid gray is the 15 min averaged fluxes.

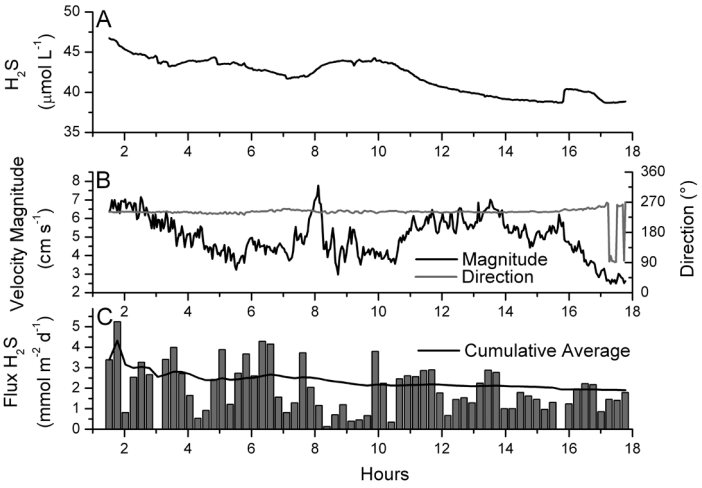

Fig. 8. H_2S EC deployment for ~18 h at 192 m water depth in the anoxic Gotland Basin (Baltic Sea). A) Evolution of H_2S_{aq} concentration over time. B) Measured horizontal velocity magnitude and direction. C) 15 min averaged ΣH_2S fluxes (bar) and the cumulative average fluxes (solid line). Light gray line indicates 2.5 min resolved fluxes used for the 15 min average.

The ΣH_2S fluxes (total sulfide) are also very intermittent during the measurement period, ranging from 0 up ~5 mmol m^{-2} d^{-1} using the 15-min bin-average, with much more variability using the 2-min flux extraction. The solid line on Fig. 8C is the cumulative average of the EC ΣH_2S flux. The mean flux over the time series is 1.9 ± 1.2 mmol m^{-2} d^{-1}. Two benthic ΣH_2S chamber deployments close by provided very similar flux values of 1.9 and 3.5 mmol m^{-2} d^{-1}, respectively (S. Sommer pers. comm.). The results of our field assessments validate the use of our amplifier for both in situ O_2 and H_2S flux measurements in benthic environments.

Discussion

The self-contained amplifier is designed to directly plug into any ADV that can record an analog input (and other ADVs) and does not use control units or signal pre-processing. The presented amplifier, unlike the commercially available highly engineered systems, is simple in design and concept. This minimizes cable lengths (potential source of noise) and eliminates any synchronization issues between the velocity and concentration data. These variables must be aligned perfectly in time to avoid distortion of the subsequent flux calculation. The signal is directly read into the ADV files and stored on the internal memory. It is recommended to use a separate power source for the amplifier independent of the ADV to minimize any potential noise (or drift) problems using a single power source for both instruments.

The same amplifier can readily accept both O_2 and H_2S microelectrodes, and could in fact be used with other amperometric microelectrodes with respect to eddy correlation; the limitation is the size and response time of the sensors. It is worth noting that the amplifier could also be used for microprofiling within the sediment. The sensitivity analyses of the amplifier performance, response time testing, and extensive data sets show that this amplifier is extremely adept at accurately capturing high-resolution O_2 and H_2S readings and their high-frequency fluctuations. Reassuring are also the data shown in Fig. 7A where the concentration was recorded with simultaneously deployed O_2 sensors with excellent agreement.

The amplifier's default configuration (see Web Appendix) includes a 1-pole (first order) filter and has low sensitivity to 50/60 Hz interference from indoor electrical sources. However, the amplifier board layout has been designed to readily receive an additional embed 2-pole filter (second order), providing up to an overall third-order filter to further reduce noise for laboratory and flume applications. However, with shielded cables, steel amplifier housing, and proper grounding (such as the grounding wires of laboratory power systems) the amplifier receives nearly negligible interference levels and allows very reliable indoor measurements even without the additional filters.

The results of Figs. 7 and 8 show a lot of variation in the fluxes. As the method resolves the flux due to turbulent eddies, it is expected that a large variability is present in the system on a short time scale. These are not variations due to "noise" in the classical sense, but are a direct result of the intermittent nature of turbulence and inherent characteristics of the approach and should help to provide new insight into benthic-boundary layer dynamics and sediment exchange phenomena.

Comments and recommendations

There are still relatively few EC studies present in the literature. With much to be gained with potential future applications, the availability and cost of the equipment should not be the limitation. With the work presented here, an easy, inexpensive, flexible, and robust solution for sensor amplification becomes available. The presented amplifier is relatively simple to build and use and will help fill a much needed demand for this exciting, and promising measuring approach. However, it is essential that the amplifier should be constructed with the highest quality components and as clean as possible to maintain the high performance of the design. To maximize both the confidence in the data sets and the likelihood that data are obtained, it is advantageous to simultaneously deploy two sensors in the same measurement volume.

As O_2 (and H_2S) EC in aquatic environments is still a relatively new technique, there are still many unknowns and uncertainties with respect to data treatment and handling, and a deeper understanding of what is actually measured. Now with the equipment in place and available, these issues can be further addressed by a broader community. The amplifier was developed as an "open-source" project and the detailed schematics are given in the Web Appendix.

References

Berg, P., H. Røy, F. Janssen, V. Meyer, B. B. Jørgensen, M. Hüttel, and D. de Beer. 2003. Oxygen uptake by aquatic sediments measured with a novel non-invasive eddy-correlation technique. Mar. Ecol.-Prog. Ser. 261:75-83 [doi:10.3354/meps261075].

———, H. Røy, and P. L. Wiberg. 2007. Eddy correlation flux measurements: The sediment surface area that contributes to the flux. Limnol. Oceanogr. 52:1672-1684 [doi:10.4319/lo.2007.52.4.1672].

———, and M. Huettel. 2008. Monitoring the seafloor using the noninvasive eddy correlation technique: Integrated benthic exchange dynamics. Oceanography 21:164-167.

———, R. N. Glud, A. Hume, H. Stahl, K. Oguri, V. Meyer, and H. Kitazato. 2009. Eddy correlation measurements of oxygen uptake in deep ocean sediments. Limnol. Oceanogr. Methods 7:576-584 [doi:10.4319/lom.2009.7.576].

Brand, A., D. F. McGinnis, B. Wehrli, and A. Wüest. 2008. Intermittent oxygen flux from the interior into the bottom boundary of lakes as observed by eddy correlation. Limnol. Oceanogr. 53:1997-2006 [doi:10.4319/lo.2008.53.5.1997].

Glud, R. N., P. Berg, A. Hume, P. Batty, M. E. Blicher, K. Lennert, and S. Rysgaard. 2010. Benthic O2 exchange across hard-bottom substrates quantified by eddy correlation in a sub-Arctic fjord. Mar. Ecol. Progr. Ser. 417:1-12 [doi:10.3354/meps08795].

Hume, A. C., P. Berg, and K. J. McGlathery. 2011. Dissolved oxygen fluxes and ecosystem metabolism in an eelgrass (Zostera marina) meadow measured with the eddy correlation technique. Limnol. Oceanogr. 56:86-96 [doi:10.4319/lo.2011.56.1.0086].

Kuhl, M., C. Steuckart, G. Eickert, and P. Jeroschewski. 1998. A H2S microsensor for profiling biofilms and sediments: application in an acidic lake sediment. Aquat. Microb. Ecol. 15:201-209 [doi:10.3354/ame015201].

Kuwae, T., K. Kamio, T. Inoue, E. Miyoshi, and Y. Uchiyama. 2006. Oxygen exchange flux between sediment and water in an intertidal sandflat, measured in situ by the eddy-correlation method. Mar. Ecol.-Prog. Ser. 307:59-68 [doi:10.3354/meps307059].

Lee, X., W. Massman, and B. Law. 2004. Handbook of micrometeorology: a guide for surface flux measurement and analysis. Kluwer Academic Publishers.

Lorrai, C., D. F. McGinnis, P. Berg, A. Brand, and A. Wüest. 2010. Application of oxygen eddy correlation in aquatic systems. J. Atmos. Oceanic Technol. 27:1533-1546 [doi:10.1175/2010JTECHO723.1].

McGinnis, D. F., P. Berg, A. Brand, C. Lorrai, T. J. Edmonds, and A. Wüest. 2008. Measurements of eddy correlation oxygen fluxes in shallow freshwaters: Towards routine applications and analysis. Geophys. Res. Lett. 35:L04403 [doi:10.1029/2007GL032747].

Revsbech, N. P. 1989. An oxygen microsensor with a guard cathode. Limnol. Oceanogr. 34:474-478 [doi:10.4319/lo.1989.34.2.0474].

Submitted 16 January 2011
Revised 28 May 2011
Accepted 28 June 2011